Uncoupling of the transactivation and transrepression functions of PARP1 protein

Elena Kotova, Michael Jarnik, and Alexei V. Tulin[1]

Epigenetics and Progenitor Cells Program, Fox Chase Cancer Center, Philadelphia, PA 19111

Edited* by Allan C. Spradling, Carnegie Institution of Washington, Baltimore, MD, and approved February 25, 2010 (received for review December 8, 2009)

Poly(ADP ribose) polymerase 1 (PARP1) is a nuclear protein that regulates chromatin remodeling and transcription as well as DNA repair and genome stability pathways. Recent studies have revealed a paradoxical dual role of PARP1 protein in transcription. Specifically, although PARP1 controls transcriptional activation of a subset of genes that are heat shock- or hormone-dependent, it also directly inactivates transcription, establishes heterochromatin domains, and silences retrotransposable elements. However, the domains required for these disparate functions are currently unknown. In this paper, we report the discovery of a previously undescribed mutation in the *Drosophila Parp* locus. We show that the mutants express a deletion mutant of PARP1 protein with an altered DNA binding domain that carries only the second Zn-finger. We demonstrate that this alteration specifically excludes PARP1 protein from heterochromatin and makes PARP1 unable to maintain repression of retrotransposable elements. By characterizing the biological activity of this unique PARP1 mutant protein isoform, we have uncoupled the transactivation and transrepression functions of this protein.

chromatin | poly(ADP ribose) polymerase | transcription

Poly(ADP ribose) polymerase 1 (PARP1) protein has been known for decades as a nuclear protein that recognizes and binds nicks and ends of DNA and catalyses poly(ADP ribose) (pADPr) synthesis (1). The basic enzymatic reactions catalyzed by PARP1 involve transferring ADPr from nicotinamide–adenine dinucleotide to either a protein acceptor or an existing pADPr chain, the average length of which is 80 or more residues (2). PARP1 protein can modify numerous chromatin proteins in vivo and in vitro (3). A key role of PARP1 was shown in DNA repair and apoptosis (3), where PARP works as a trigger between the DNA repair (4) and apoptotic pathways (5). PARP1 enzymatic activity has also been shown to be required for normal assembly of higher order chromatin structures and for transcriptional activation (6). Moreover, it has been shown that PARP1 regulates the transcription of these genes by inducing chromatin loosening at targeted genetic loci (6, 7). Finally, PARP1 establishes silent chromatin domains and represses retrotransposable elements (8).

The characterization of deletion mutants of PARP that distinguish among the varied functions of this protein is essential to establish a more complete understanding of PARP1 protein biology. At present, however, we have identified neither the mechanism of PARP protein targeting to specific chromatin domains nor the mechanism of local PARP activation. Closing these gaps in our current knowledge is complicated because the presence of 18 paralogous PARP proteins (9) in mammals most likely results in corresponding functional redundancies. The *Drosophila* genome (8, 10, 11) encodes only a single nuclear PARP (PARP1), making this animal an invaluable model system for the study of PARP functions.

The PARP1 protein has three functionally defined domains conserved from human to *Drosophila* (12, 13): (*i*) an N-terminal DNA binding domain (DBD) encompassing two Zn-fingers, which recognizes DNA lesions; (*ii*) a centrally localized automodification domain (AD), which can be modified by ADPr and is also required for dimerization; and (*iii*) a C-terminal catalytic domain, which performs ADPr transfer (Fig. 1*A*). Zn-finger 2 of PARP1 was shown to be critical for the recognition and binding of DNA breaks in vitro (14), whereas a role in stabilization of established interaction was suggested for Zn-finger 1 (3). Recently, the DBD and, specifically, the Zn-fingers were suggested to control PARP1-dependent chromatin condensation (15). Here, we report the discovery of a unique *C03256* pBac element-mediated mutation in the *Drosophila Parp* locus that leads to expression of a truncated mutant of PARP1 ($PARP^{\Delta 300}$) (Fig. 1*A*). $PARP^{\Delta 300}$ lacks the first Zn-finger of the DBD, enabling us to elucidate the in vivo function of Zn-finger 1 and the effect that this unique PARP1 deletion mutant has on chromatin and PARP1-dependent nuclear processes. We find that this mutation uncouples the transactivation and transcriptional repression functions of PARP.

Results

$parp^{C03256}$ Has Residual Poly(ADP Ribosyl)ation Activity in Chromatin. Previously, we described a P element-mediated mutation, $parp^{CH1}$, which impairs expression of a single *Drosophila parp* gene in embryos. Localization of the $parp^{CH1}$ element in the remote upstream promoter region, which spans more than 100 kb of transposon-rich centromeric heterochromatin (Fig. 1*B*), causes developmental arrest in *Drosophila* at ecdysis II stage and lethality, which precludes the study of PARP protein function late in the development in this mutation. To find unique mutations in the *parp* gene, we analyzed the Exelexis collection of pBac element-induced mutations in this gene (16). Sequence identity was observed for the 3′-end flanking sequence of the *C03256* insertion site and exon 4 of the PARP1 coding sequence (Fig. S1 *A* and *B*). To confirm the *C03256* insertion site, we performed Southern blot analysis of genomic DNA from WT and *C03256* homozygous flies using PARP1 cDNA as a probe. We found that insertion of the *C03256* element changed the pattern of Parp-specific genomic DNA digestion, as expected, based on the computer-generated map (Fig. S1 *B* and *C*). To test whether *C03256* disrupts transcription of the *Parp* locus, we performed RT-PCR analysis. We found that *Parp* expression is completely abolished in the region of exons 3–5, which encode the Zn-finger 1 of PARP1 protein (Fig. 1*C*). Surprisingly, we found that *C03256* mutants accumulate a low but detectable amount of *Parp* RNA encoded by exons 5–8 (Fig. 1*C*). Taken together, these findings define *C03256* as a previously undescribed hypomorphic mutation in the *Drosophila Parp* locus and suggest that transcription in homozygous *C03256* starts from a cryptic promoter, which we denote as Pm3 (Fig. 1*B*).

To analyze this mutation in the *Parp* locus further, we characterized *C03256* viability. Although 27% of *C03256* mutant animals survived up to pupae, most homozygous *C03256* animals died at the second and third larval stages (Table S1). Precise excision of the *C03256* pBac element generated 100% viable stocks, arguing

Author contributions: E.K., M.J., and A.V.T. designed research; E.K., M.J., and A.V.T. performed research; E.K. and A.V.T. contributed new reagents/analytic tools; E.K. and M.J. analyzed data; and E.K. and A.V.T. wrote the paper.

The authors declare no conflict of interest.

*This Direct Submission article had a prearranged editor.

[1]To whom correspondence should be addressed. E-mail: alexei.tulin@fccc.edu.

This article contains supporting information online at www.pnas.org/cgi/content/full/0914152107/DCSupplemental.

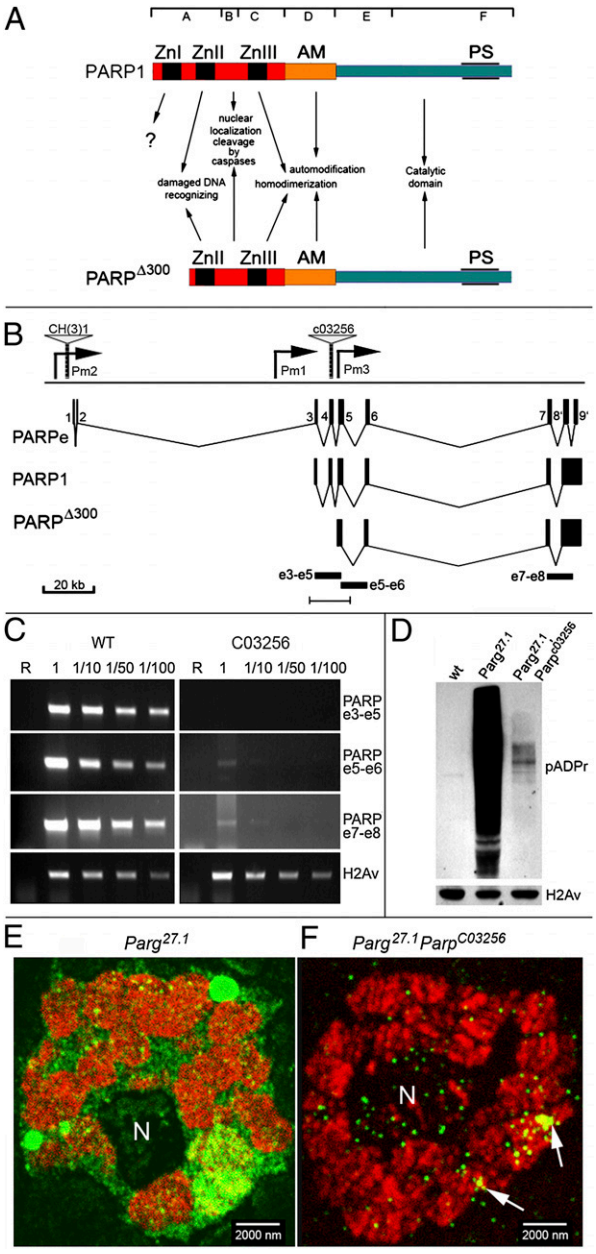

Fig. 1. (*A*) Domain structure comparison for PARP1 protein and PARP$^{\Delta300}$ protein isoform. (*Top*) Subdivision on seven domains (A–F) is shown according to D'Amours et al. (3). (*Middle*) Known functions of domains are indicated. ZnI, ZnII, and ZnIII correspond to Zn-finger domains. AM, automodification domain; PS, PARP signature, evolutionarily conserved PARP catalytic site. (*B–F*) C03256 mutation disrupts PARP expression. (*B*) Structure of *Drosophila Parp* locus. A diagram summarizing the organization of the *Parp* genomic region as determined from this and a previous study (8) is shown. Gray triangles indicate mobile element insertions disrupting locus CH(3)1 (8) and C03256. Pm1 and Pm2 indicate promoters reported previously (8), and Pm3 indicates a presumptive promoter, as suggested from this study. The arrangement of the exons, as described in the article by Tulin et al. (8), encoding a naturally occurring catalytically inactive PARPe (*Upper*) and full-length catalytically active PARP1 (*Lower*) is shown. Black rectangles e3–e5, e5–e6, and e7–e8 indicate PCR fragments used to show disruption of PARP transcription in *C*. The bar at the bottom indicates the region that is magnified in Fig. S1*B*. (*C*) C03256 disrupts PARP transcription; RT-PCR analysis of WT and C03256 mutant flies. R, RNA; 1, 1/10, 1/50, 1/100, dilutions of RNA sample before cDNA synthesis. Specific primers to exons 3 and 5 (PARP e3–e5), exons 5 and 6 (PARP e5–e6), and exons 7 and 8 (PARP e7–e8) were used. Specific primers to H2Av transcript were used as a loading control. The *C03256* disrupts transcription completely in the region of exons 3–5, but a low amount of mRNA specific to exons 5–8 is still detected, strongly that the *C03256* element is responsible for the original lethality.

We next sought to verify that the *C03256* mutation could be rescued by expression of a WT PARP cDNA transgene or by suppression of the activity of the PARP antagonist poly(ADP ribose) glycohydrolase (PARG), which is responsible for cleavage of pADPr (17, 18). For the first approach, we expressed previously verified (6, 18, 19) UAS::PARP1-DsRed and UAS::PARP embryonic (PARPe)-EGFP transgenic constructs with G1-Gal4 ubiquitous driver. Ectopic expression of full-length PARP1 protein (PARP1-DsRed) but not the catalytically inactive PARPe protein (PARPe-EGFP) rescues *C03256* lethality completely (Table S2). Mutant *Drosophila* bearing a single copy of PARP1-DsRed and G1-Gal4 driver can be readily maintained as homozygous stock (*Gal4^{G1}, UAS::PARP1-DsRed/FM7i; parp^{C03256}/parp^{C03256}*). The ability of PARP1-DsRed expression to rescue *C03256* mutants completely demonstrates that the *C03256* element directly disrupts the *Parp* gene. We will therefore call the *C03256* allele *parp^{C03256}* in the following text. For the second approach, we found that reduction of PARG protein activity in the *parg$^{27.1}$/FM7i; parp^{C03256}/parp^{C03256}* animals also partially rescues *C03256* lethality (Table S2). This finding supports the premise that *parp^{C03256}* is a nonnull (hypomorphic) mutation and that residual activity of PARP is sufficient for animals to survive if PARG function is partially suppressed.

The absence of antibodies against *Drosophila* PARP proteins complicates the quantification of PARP1 function reduction in *parp^{C03256}* animals. However, PARP protein is a pADP ribosylating enzyme, allowing us to immunoblot for pADPr to detect levels of PARP protein enzymatic activity in *parp^{C03256}* animals. We previously demonstrated significant reduction of the pADPr level in *parp^{C03256}* flies when compared with WT flies (20 [figure 5a], 21). Small levels of activity can be seen when PARG is reduced because it catalyzes the opposite reaction (Fig. 1*D*, second lane). Examination of *parp^{C03256}* in a PARG mutant background revealed enzymatic activity in the mutant (Fig. 1*D*, third lane). Thus, PARP1 protein enzymatic activity is certainly present in *parp^{C03256}* mutants, and the amount of this activity correlates with the amount of residual PARP RNA detected, as shown in Fig. 1*C*. To localize this activity in situ, thick sections of third-instar larvae salivary gland nuclei were immunostained with anti-pADPr antibodies. We compared nuclear pADPr in *parg$^{27.1}$* and *parg$^{27.1}$; parp^{C03256}* using confocal microscopy. Despite a dramatic reduction of the pADPr signal (Fig. 1*D*) by immunoblot analysis, the residual pADPr had proper localization in specific domains of chromatin (Fig. 1 *E* and *F* and Fig. S1*D*), suggesting that the residual PARP protein in *parp^{C03256}* localizes to chromatin and nucleoli in a pattern that is similar to PARP1 protein in WT flies.

***parp^{C03256}* Mutants Express a Short PARP1 Protein Isoform, PARP$^{\Delta300}$, Which Encodes PARP1 Protein Without the Zn-Finger 1 Domain.** To characterize the PARP1 protein isoform that is expressed in *parp^{C03256}*, we cloned PARP cDNAs from *parp^{C03256}* homozygous larvae using an RT-PCR approach. A single cDNA for Parp$^{\Delta300}$ was identified (Fig. S2*A*). RT-PCR experimentation demonstrated that the start of transcription in *parp^{C03256}* occurs downstream

suggesting an additional start of transcription downstream from C03256. (*D*) Western blots of proteins isolated from third-instar larvae of WT (wt), *Parg$^{27.1}$* mutant, and *Parg$^{27.1}$, Parp^{C03256}* double-mutant animals probed with anti-pADPr antibody. C03256 suppresses the accumulation of pADPr in *Parg* mutants. An antihistone H2Av antibody was used as a loading control. (*E* and *F*) Immunofluorescent detection of pADPr accumulation is shown in salivary gland nuclei of *Parg$^{27.1}$* mutant and *Parg$^{27.1}$, Parp^{C03256}* double-mutant animals. Rabbit anti-pADPr antibody was used (green). To stain chromatin, mouse anti-^{1}H histone antibody was used (red).

from the pBac element 3′ end, inside of intron 4, and that Parp$^{\Delta 300}$ cDNA includes PARP1 protein-encoding exons 5–8 (Fig. S2*A*). The analysis of the Parp$^{\Delta 300}$ cDNA sequence reveals three putative ORFs that encode PARP (Fig. S2*A*). The longest ORF, PΔ300, starts in intron 4 and carries all domains of PARP1 except the Zn-finger 1 (Fig. S2 *A* and *B*). Another two putative ORFs (PΔ740 and PΔ1302) encode shorter polypeptides without nuclear localization signals. To validate the biological properties of the predicted PARP protein isoforms, we generated transgenic flies that express each ORF fused to EYFP (Fig. S2*B* and *Materials and Methods*). We studied the localization of those recombinant PARP proteins throughout many tissues in WT and *parp*^{C03256} flies (Fig. S2 *C–E*). Only PARP$^{\Delta 300}$-EYFP protein localized to chromatin and nucleoli (Fig. S2*C*), whereas other recombinant proteins are excluded from chromatin (PARP$^{\Delta 1302}$-EYFP) (Fig. S2*D*) or completely removed from nuclei (PARP$^{\Delta 740}$-EYFP) (Fig. S2*E*). Ubiquitous expression of PARP$^{\Delta 300}$-EYFP partially rescues *parp*^{C03256} viability (Table S2), although the other two proteins do not rescue *parp*^{C03256}. This suggests that the main reason for *parp*^{C03256} lethality is an insufficient amount of PARP protein. Together, our results support the idea that PARP$^{\Delta 300}$ protein is produced and functional in *parp*^{C03256} mutants.

PARP$^{\Delta 300}$ Protein Is Activated by γ-Irradiation and Is Sufficient for the Genotoxic Stress Response. The earliest known PARP1 protein function was to protect the genome from genotoxic stresses such as irradiation (3). PARP1 protein is known to be activated on the appearance of DNA damage (3), and the PARP1-dependent pADPr reaction has been shown to be critical for proper DNA repair (4) and genome stability (22). Thus, to examine the biological properties of PARP$^{\Delta 300}$ protein and *parp*^{C03256} mutation, we analyzed the genotoxic stress response of *parg*$^{27.1}$*; parp*^{C03256} double-mutant animals, which express only PARP$^{\Delta 300}$-like protein. We compared genotoxic responses in *parg*$^{27.1}$*; parp*^{C03256} mutants with those in WT flies and *parg*$^{27.1}$ mutants alone. First, we found that on irradiation, both *parg*$^{27.1}$*; parp*^{C03256} and *parg*$^{27.1}$ were able to increase the amount of pADPr (Fig. S3*A*). Thus, full-length WT PARP1 protein and PARP1 lacking the first Zn-finger were activated by DNA damage. Second, we compared the viability of the *parg*$^{27.1}$*/FM7i; parp*^{C03256}*/parp*^{C03256} mutants with that of their WT siblings after 36-Gy irradiation at the third-instar larval stage (Fig S3*B* and *Materials and Methods*). No significant difference was observed. These data support our conclusion that PARP$^{\Delta 300}$ protein is sufficient for viability after genotoxic stress and, as a consequence, Zn-finger 1 is not required for PARP1 protein activation on irradiation.

PARP$^{\Delta 300}$ Protein Has Similar Nuclear Dynamics Compared with PARP1. To study the nuclear dynamics of the PARP$^{\Delta 300}$-EYFP protein isoform, we first analyzed the chromosomal localization of this protein when expressed in *parp*^{C03256}. Immunostaining using anti-GFP antibody demonstrated nuclear localization and broad association with chromatin of diploid and polyploid nuclei. In vivo imaging showed that most PARP$^{\Delta 300}$-EYFP protein remains bound to chromatin in interphase nuclei and accumulates in nucleoli (Fig. 2*A*, arrows). However, a significant pool of this protein is present in soluble nucleoplasm (Fig. 2*A*, arrowheads), suggesting that there is an equilibrium of PARP$^{\Delta 300}$ protein binding to chromatin. To investigate the nuclear dynamics of this PARP isoform, we employed the fluorescence recovery after photobleaching (FRAP) approach (19). We compared the FRAP dynamics of PARP$^{\Delta 300}$-EYFP protein with those of full-length previously validated (19, 23) PARP1-DsRed in *Drosophila* polyploid nuclei. We expressed both recombinant proteins separately in *parp*^{C03256} mutant animals using the Armadillo-Gal4 driver, which is expressed ubiquitously (24). The average FRAP rates of PARP$^{\Delta 300}$-EYFP and PARP1-DsRed are not statistically different (Fig. 2*B*), suggesting that the Zn-finger 1 is not necessary for PARP protein dynamics in chromatin.

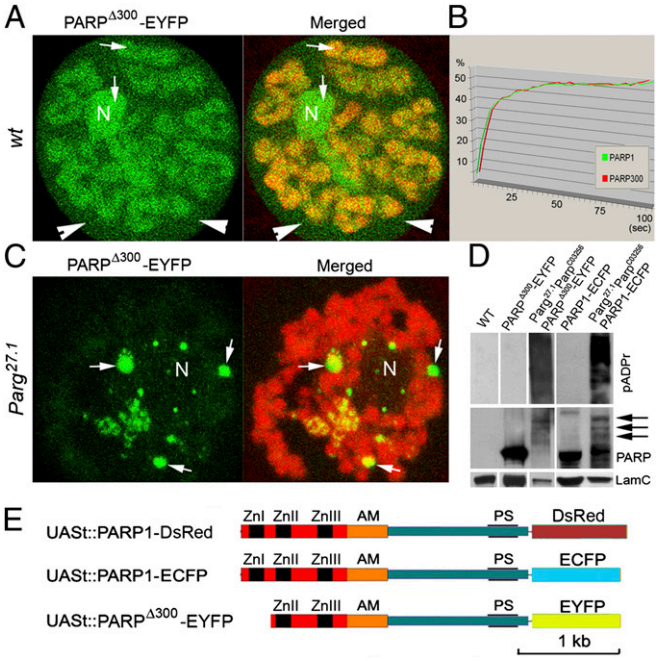

Fig. 2. PARP$^{\Delta 300}$ protein localization dynamics and enzymatic activity in vivo. (*A*) Life imaging shows ubiquitous distribution of PARP$^{\Delta 300}$-EYFP protein (green) in chromatin (red) and nucleolus (N). Arrows show presence of PARP$^{\Delta 300}$-EYFP protein in soluble nucleoplasm. (*B*) FRAP assay demonstrates similar average in vivo dynamics for PARP$^{\Delta 300}$-EYFP and PARP1-ECFP proteins. (*C*) Life imaging shows relocalization of PARP$^{\Delta 300}$-EYFP protein (green) from chromatin (red) and nucleolus (N) into nucleoplasmic bodies in *Parg*$^{27.1}$ mutants. (*D*) Western blot demonstrates automodification of PARP$^{\Delta 300}$-EYFP and PARP1-ECFP proteins in *Parg*$^{27.1}$*;Parp*^{C03256} mutant animals. The following antibodies were used: mouse anti-pADPr, rabbit anti-GFP (to detect PARP$^{\Delta 300}$-EYFP and PARP1-ECFP proteins), and mouse anti-lamin C (loading control). Positions of heavily modified forms of PARP$^{\Delta 300}$-EYFP and PARP1-ECFP proteins are shown with arrows. (*E*) Structure of UAS/Gal4-inducible transgenic recombinant PARP1-DsRed, PARP1-ECFP, and PARP$^{\Delta 300}$-EYFP proteins. The DNA-binding domain of PARP is indicated in red, the automodification (AM) domain is indicated in orange, and the catalytic domain in blue contains a PARP enzymatically active site (PS).

PARP1 protein is active as a dimer (25, 26). Covalent ADPr automodification of the PARP1 "Brca1 C-terminal" (BRCT) domain (AM) causes PARP1 dimers to dissociate from each other and from active chromatin and to lose activity (18). A cluster of 10–28 Glu residues located near the center of the PARP1 BRCT domain serves as the major acceptor of this ADPr in vivo (3). The negative feedback loop mediated by automodification limits the time during which PARP1 molecules can remain active. In *Parg* mutants, we previously showed that PARP1 protein is pADP-ribosylated and removed from chromatin into specific nucleoplasmic bodies (18, 23). To test the enzymatic activation of PARP$^{\Delta 300}$and its ability to react to automodification, we expressed the PARP$^{\Delta 300}$-EYFP transgene in *parg*$^{27.1}$*; parp*^{C03256} double mutants and analyzed PARP$^{\Delta 300}$-EYFP protein dynamics using in vivo imaging. We found that PARP$^{\Delta 300}$ protein is completely relocalized into nucleoplasmic bodies at the third-instar larvae stage (Fig. 2*C*), which is a pattern identical to what we had previously shown for full-length PARP1 protein (23). Immunoblot analysis of proteins extracted from *parg*$^{27.1}$*; parp*^{C03256} double-mutant animals expressing PARP$^{\Delta 300}$-EYFP confirmed that the PARP$^{\Delta 300}$ isoform is able to perform a pADPr reaction and could largely automodify itself (Fig. 2*D*). Taken together, our findings suggest that the Zn-finger 1 of PARP1 protein is not required for general interaction of PARP protein with chromatin or PARP enzymatic activation in vivo. Taking into account that expression of

extra-PARP$^{\Delta 300}$ is also sufficient to rescue the *parp*^{C03256} flies to viability in steady state and on irradiation, we conclude that PARP$^{\Delta 300}$ performs essentially like full-length PARP1 protein.

Deletion of the Zn-Finger 1 of PARP1 Protein Alters Specificity of Chromatin Domains Recognized by PARP Protein. To investigate the roles of Zn-finger 1 for PARP1 protein functions further, we compared the localization of PARP$^{\Delta 300}$ and PARP1 protein using high-resolution confocal microscopy of fixed whole-mount and thick-sectioned *Drosophila* tissues. For maximal elimination of artificial differences between PARP$^{\Delta 300}$ and PARP1 recombinant proteins, we used the PARP1-ECFP transgene instead of PARP1-DsRed (Fig. 2*E*). We coexpressed PARP$^{\Delta 300}$-EYFP and PARP1-ECFP in WT *Drosophila*. A significant difference in localization of those proteins was revealed (Fig. 3). Specifically, some specific domains of chromatin predominantly accumulate PARP1, but others have enriched PARP$^{\Delta 300}$ (Fig. 3 *A–C*, arrows). In general, the PARP1 isoform has more widespread distribution in chromatin (Fig. 3*C*, compare green and red channels, respectively). Coexpression of PARP$^{\Delta 300}$-EYFP and PARP1-ECFP in *parg*$^{27.1}$ mutants also revealed a difference in the targeting of those proteins into nucleoplasmic bodies (Fig. 3*D*), confirming our suggestion about broader PARP1 localization. These observations, taken together, suggest that the Zn-finger 1 of PARP1 functions to govern the binding specificity of the protein.

PARP$^{\Delta 300}$ Protein Is Enriched in Regions of Euchromatin and Is Sufficient for Heat-Shock Activation of Genes. To determine patterns of PARP1-ECFP and PARP$^{\Delta 300}$-EYFP localization in chromatin, we compared the localization of these proteins on *Drosophila* salivary gland polytene chromosomes (Fig. 4 *A* and *B*). Both proteins show broad but distinct distribution along chromosomes. PARP1-ECFP protein shows significant accumulation in regions of inactive condensed chromatin with high DNA content (Fig. 4*A*, arrows). The PARP$^{\Delta 300}$-EYFP protein, however, is excluded from "dense" chromatin and accumulates in decondensed loci (with low DNA content) (Fig. 4*B*, arrows). This observation suggests that PARP1 and PARP$^{\Delta 300}$ proteins have different mechanisms of targeting to chromatin and that the Zn-finger 1 domain of PARP1 protein controls one of those.

To examine the pattern of PARP1 and PARP$^{\Delta 300}$ protein binding in active chromatin, we performed ChIP experiments. Previously, we demonstrated that PARP controls heat shock response and activation of hsp70 expression (6). Subsequently,

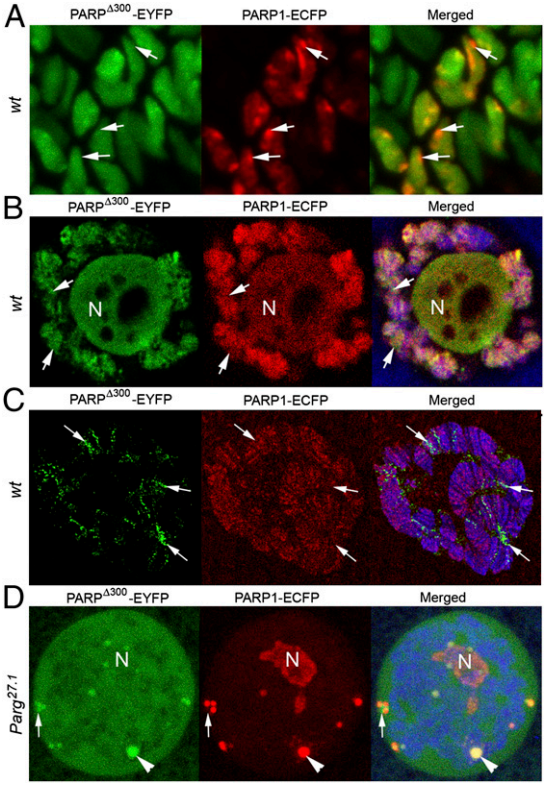

Fig. 3. PARP$^{\Delta 300}$ and PARP1 proteins have a different localization in chromatin. High-resolution confocal microscopy of fixed tissues reveals differences in PARP$^{\Delta 300}$-EYFP and PARP1-ECFP protein localization and dynamics in chromatin in WT whole-mount preparations (*A* and *B*) and thick-section samples (*C*) as well as in *Parg*$^{27.1}$ mutant animals (*D*). The difference between PARP1-ECFP and PARP$^{\Delta 300}$-EYFP localization in chromatin and Cajal bodies is maximal in the regions labeled with arrows. Larval imaginal disks (*A*) and salivary glands (*B–D*) were dissected from UAS::PARP1-ECFP, Arm::Gal4; *Parp*^{C03256}/*Parp*^{C03256} and UAS::PARP$^{\Delta 300}$-EYFP, Arm::Gal4; *Parp*^{C03256}/*Parp*^{C03256} animals. (*C*) Fine-frozen sections of salivary gland were prepared and stained with anti-^{1}H antibody to detect chromatin (blue). PARP1-ECFP (red) and PARP$^{\Delta 300}$-EYFP (green) protein localization was detected by autofluorescence of ECFP and EYFP.

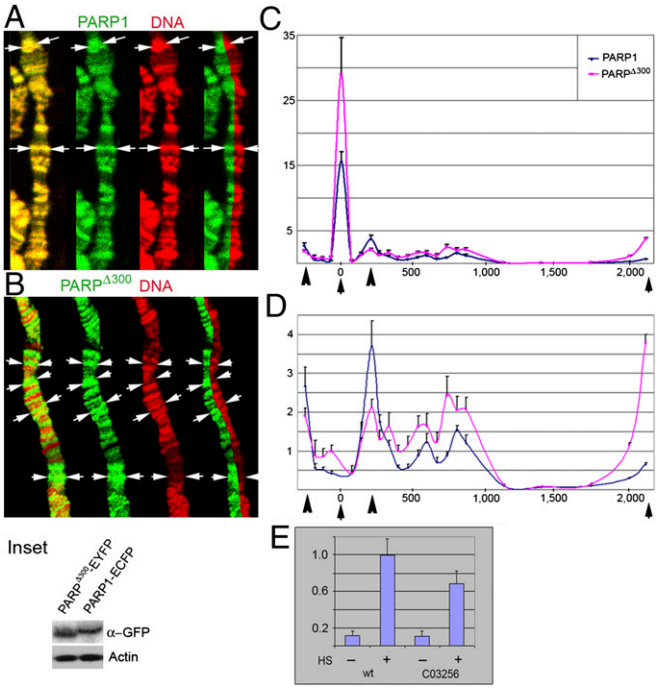

Fig. 4. PARP$^{\Delta 300}$ protein preferentially localizes into domains of euchromatin. A comparison of PARP1 and PARP$^{\Delta 300}$ protein localization in salivary gland polytene chromosomes is shown. Salivary glands were dissected from UAS::PARP1-ECFP, Arm::Gal4; *Parp*^{C03256}/*Parp*^{C03256} (*A*) or UAS::PARP$^{\Delta 300}$-EYFP, Arm::Gal4; *Parp*^{C03256}/*Parp*^{C03256} (*B*) third-instar larvae, squashed on slides, and immunostained with anti-GFP antibody (green). DNA is shown in red. PARP1 protein shows significant localization with DNA (condensed heterochromatic regions) (*A*), whereas PARP$^{\Delta 300}$ localizes preferentially in regions of decondensed chromatin (euchromatin) (*B*). (*Inset*) Arrows indicate regions of PARP protein enrichment. The expression level of PARP$^{\Delta 300}$-EYFP and PARP1-ECFP recombinant proteins is compared. (*C* and *D*) ChIP assay demonstrates that the hsp70 locus accumulates significantly more PARP$^{\Delta 300}$ protein than PARP1. (*C*) Distribution of PARP$^{\Delta 300}$ (red) and PARP1 (blue) proteins along the hsp70 gene. PARP$^{\Delta 300}$ shows significant enrichment in the regions of transcriptional start and termination (black arrows). Arrowheads indicate positions of nucleosomes −1 and +1. (*D*) For better representation of PARP protein localization in the body of the hsp70 gene, we include the same ChIP experimental data with depleted point "0." (*E*) C03256 mutation does not block hsp70 gene activation. The quantitative RT-PCR assay using primers specific to Hsp70 cDNA detects only 30% less Hsp70 mRNA in *Parp*^{C03256} mutants than in WT flies.

GENETICS

binding of PARP and its enzymatic activation were shown to be critical for Pol2 polymerase-dependent transcription within the Hsp70 gene (7, 27). Here, we compared distribution of PARP1-ECFP and PARP$^{\Delta 300}$-EYFP proteins along the hsp70 locus in *parp*^{C03256} mutants. To detect hsp70 DNA in ChIP experiments, we used 24 pairs of primers distributed along 3 kb of the hsp70 genomic sequence (base pairs −500 to +2,500 relative to transcriptional start) (Fig. 4 *C* and *D*). Although both PARP isoforms were enriched at the transcriptional start and termination as they distributed among nucleosomes at the 5′ end of the hsp70 sequence, they were depleted from the second half of the locus (Fig. 4 *C* and *D*). PARP$^{\Delta 300}$, however, demonstrated much higher accumulation at transcriptional start and termination sites (Fig. 4 *C* and *D*, arrows). These data support the observation that deletion of Zn-finger 1 facilitates accumulation in active chromatin.

To explore the functional differences of PARP1 and PARP$^{\Delta 300}$ proteins in transcription, we compared transcriptional activation between hsp70 genes in WT *Drosophila* larvae and *parp*^{C03256} mutants, which express only PARP$^{\Delta 300}$ protein. We found that *parp*^{C03256} mutants could activate expression of hsp70 on 30 min of heat shock (Fig. 4*E*). The hsp70 mRNA production, which was reduced by 25%, could be explained by the reduced level of total PARP protein in the mutant (Fig. 1 *C* and *D*). Moreover, expression of the PARP$^{\Delta 300}$-EYFP transgene rescues hsp70 transcription in *parp*^{C03256} mutants completely. Collectively, our results again support the conclusion that PARP$^{\Delta 300}$ protein is fully functional PARP and that Zn-finger 1 is only required for fine-tuning of PARP protein localization in the genome.

Zn-Finger Domain 1 Is Necessary for the Silencing of Retrotransposable Elements. We previously showed that PARP1 protein is required for silencing of heterochromatic repeated DNAs (8). This, along with our current observation that PARP$^{\Delta 300}$ is absent from condensed chromatin domains, suggests that Zn-finger 1 may target PARP1 to loci that should be silent. We examined localization of PARP1-ECFP and PARP$^{\Delta 300}$-EYFP in heterochromatin using immunostaining of *Drosophila* polytene chromosomes and ChIP approaches. Although PARP1 protein shows significant accumulation in both constitutive (Fig. 5*A*, arrowhead) and intercalary (Fig. 5*A*, arrows) heterochromatin, PARP$^{\Delta 300}$ protein is excluded from both (Fig. 5*B*). At the same time, PARP1 protein is enriched on sequences of retrotransposable elements *copia* and *gypsy* (typical content of silent chromatin), whereas the amount of PARP$^{\Delta 300}$ is diminished (Fig. 5*C*). Moreover, we found that *parp*^{C03256} mutants expressing PARP$^{\Delta 300}$ but not PARP1 dramatically overproduce mRNA of both retrotransposons (Fig. 5 *D* and *E*) and accumulate retroviral particles in nucleoplasm (Fig. 5 *F–H*). These phenotypes could be rescued by PARP1 expression but not by PARP$^{\Delta 300}$. Thus, we conclude that disruption of the Zn-finger 1 domain abolishes proper targeting of PARP1 to heterochromatin and leads to the desilencing of retrotransposable elements.

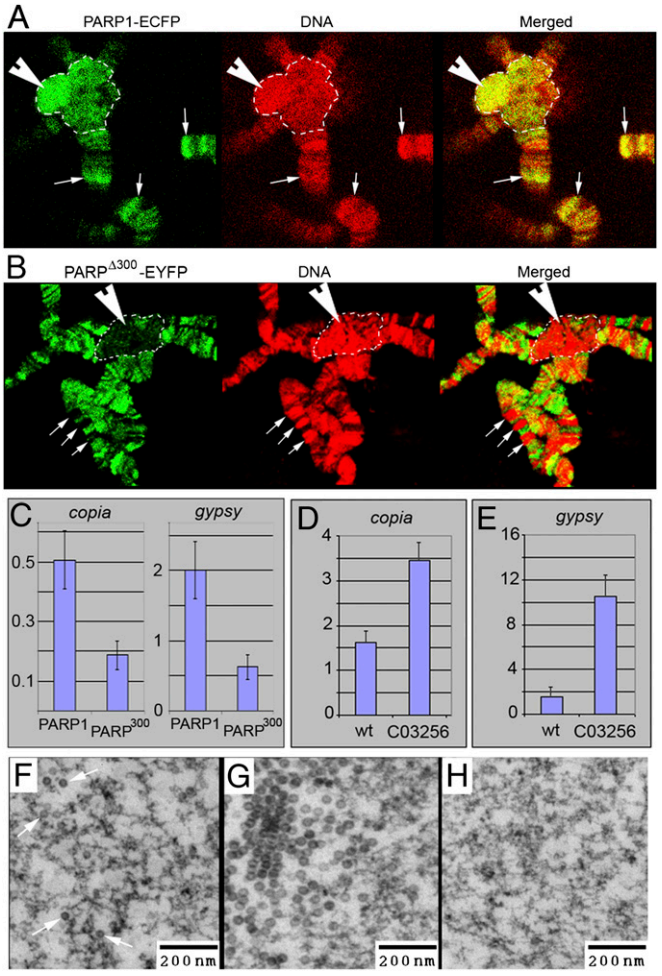

Fig. 5. PARP$^{\Delta 300}$ protein is excluded from the regions of heterochromatin. (*A* and *B*) Comparison of PARP1 and PARP$^{\Delta 300}$ protein localization in salivary gland polytene chromosomes. Salivary glands were dissected from UAS::PARP1-ECFP, Arm::Gal4; *Parp*^{C03256}/*Parp*^{C03256} (*A*) or UAS::PARP$^{\Delta 300}$-EYFP, Arm::Gal4; *Parp*^{C03256}/*Parp*^{C03256} (*B*) third-instar larvae, squashed on slides, and immunostained with anti-GFP antibody (green). DNA is shown in red. PARP1 protein shows significant accumulation in the regions of constitutive (arrowhead) and intercalary (arrows) heterochromatin (*A*), whereas PARP$^{\Delta 300}$ is excluded from these regions (*B*). Constitutive heterochromatin is indicated with a dashed line. (*C*) ChIP assay demonstrates that chromatin of retrotransposons *copia* and *gypsy* accumulates significantly less PARP$^{\Delta 300}$ protein than PARP1. (*D–H*) C03256 mutation disrupts silencing of retrotransposons. The quantitative RT-PCR assay using primers specific to *copia* (*D*) and *gypsy* (*E*) retrotransposons detects an elevated level of their RNA in *Parp*^{C03256} mutant larvae compared with heterozygous animals. EM microphotographs reveal the accumulation of retroviral particles in the nucleoplasm of *Parp*^{C03256} animals: individual particles (*F*) and clusters (*G*). (*H*) Silencing of retrotransposons could be restored by PARP1-DsRed expression.

Discussion

PARP1 is the second most abundant nuclear nonhistonic protein. The distribution of PARP1 in chromatin is nonrandom, occurring in characteristic profiles specific for distinct cell types (28–31). At present, however, the molecular basis for PARP1 binding to chromatin remains poorly understood. Here, we described a *Drosophila* mutant, which expresses a short isoform of PARP1 protein without Zn-finger 1. We discovered that mutating Zn-finger 1 does not affect average mobility of PARP protein in chromatin but that it does abolish localization of PARP protein in heterochromatin and increase accumulation of PARP in euchromatic loci. This observation suggests that the N-terminal domain of PARP1 is necessary for suppressing the binding of PARP1 to some affinity chromatin sites specifically related to retrotransposable DNA.

The molecular basis for PARP1 binding to chromatin remains poorly understood. Zn-finger 1 may contribute to the direct recognition of DNA sequences specific for heterochromatin. Such a sequence could be part of the genome of retrotransposable elements. The ability to bind sequence TGTTG has been previously reported for mammalian PARP1 (32). Sequence TGTTG is known to be an evolutionarily conserved flanking sequence for many retroviral and retrotransposable elements with long terminal repeats, such as *copia* and *gypsy* in *Drosophila*. Therefore, Zn-finger 1 may control direct binding of PARP1 protein to these high-affinity sites, followed by redistribution into surrounding chromatin.

Alternatively, Zn-finger 1 may interact with a specific chromatin protein or with a specific modification of an abundant chromatin

protein rather than directly with DNA. Considerable evidence suggests that PARP1 directly interacts with histones (3). For example, histones H1, H2A, and H2B are preferential targets for PARP1 binding in vitro (33), and they are enzymatically modified by PARP1 (34–36). However, *Drosophila* histone H1 was recently reported as an antagonist of PARP1 binding to chromatin (28). To date, of all the PARP1 interactors identified through in vitro experiments, none shows significant colocalization with PARP1 in chromatin. Therefore, it is clear that the chromatin components that are responsible for PARP1 targeting have not yet been identified.

Another possible explanation of the effects of Zn-finger 1 deletion on PARP interaction with chromatin could be that Zn-finger 1 interacts with other PARP1 domains and masks them from the recognition of high-affinity sites in chromatin. This suggestion is supported by our previous observation, wherein we demonstrated in vitro that the N-terminal domain of PARP1 suppresses interaction of PARP1 with histones H3 and H4 (19). This might explain the enrichment of $PARP^{\Delta 300}$ in active open chromatin observed in vivo in the present work. Specifically, sites of chromatin with a high level of H3/H4 exposure in open chromatin (by nucleosome modifications) may titrate $PARP^{\Delta 300}$ protein and bind it with high affinity, although the affinity of $PARP^{\Delta 300}$ to the rest of chromatin is unchanged compared with PARP1 protein.

Collectively, our data show that the second zinc finger is sufficient for PARP1 activation, localization to active chromatin, and most PARP1 functions required for viability of the fly. Further, we demonstrate that the first zinc finger is required for PARP localization to heterochromatin, where it regulates transcriptional silencing. We can now separate PARP functions molecularly. This reagent will enable us to identify the PARP transcriptional targets required for viability.

Experimental Procedures

***Drosophila* Strains.** Flies were cultured on standard cornmeal-molasses-agar media at 22 °C unless otherwise indicated. The fly stocks were generated by standard genetic methods or obtained from the Bloomington Drosophila Stock Center and the Exelixis collection at the Harvard University Medical School. Detailed information is provided in *SI Text*.

Mononucleosome ChIP. The chromatin and PARP protein complexes were immunoprecipitated using anti-GFP rabbit polyclonal antibody (Torrey Pines Biolabs). DNA from the elutes was measured by the real-time PCR assay. Detailed information is provided in *SI Text*.

Real-Time RT-PCR Assay. RNA was reverse-transcribed, and the real-time PCR assays were performed using an ABI 7900 HT instrument (Applied Biosystems). Detailed information is provided in *SI Text*.

Online Supplemental Material. Fig. S1 describes the C03256 mutation that disrupts the PARP locus. Fig. S2 illustrates the structure of the putative PARP protein isoforms that we discovered in C03256 mutants. Fig. S3 shows that the $PARP^{\Delta 300}$ protein isoform is sufficient for *Drosophila* viability during the genotoxic stress response. *SI Text* includes supplemental experimental procedures and references.

ACKNOWLEDGMENTS. We thank Drs. G. Cavalli, A. Veraksa, P. Fisher, R. Glaser, and R. Lewis for providing materials. We also thank the Exelexis mutagenesis project for the *C03256* mutant *Drosophila* line. Drs. Maureen E. Murphy and Alana O'Reilly contributed valuable comments on the manuscript. We also thank Corinne Stobbe for assistance with irradiation experiments. Quantitative RT-PCR analysis was provided by Dr. Emmanuelle Nicolas of the Fox Chase Cancer Center Genomics Facility. The research was supported by grants from the National Institutes of Health (R01 GM077452) and the Ellison Medical Foundation (GM27875) (to A.V.T.).

1. De Murcia G, Shall S (2000) *From DNA Damage and Stress Signaling to Cell Death Poly (ADP-Ribosylation) Reactions* (Oxford Univ Press, New York).
2. Rippmann JF, Damm K, Schnapp A (2002) Functional characterization of the poly(ADP-ribose) polymerase activity of tankyrase 1, a potential regulator of telomere length. *J Mol Biol* 323:217–224.
3. D'Amours D, Desnoyers S, D'Silva I, Poirier GG (1999) Poly(ADP-ribosyl)ation reactions in the regulation of nuclear functions. *Biochem J* 342:249–268.
4. El-Khamisy SF, Masutani M, Suzuki H, Caldecott KW (2003) A requirement for PARP-1 for the assembly or stability of XRCC1 nuclear foci at sites of oxidative DNA damage. *Nucleic Acids Res* 31:5526–5533.
5. Andrabi SA, et al. (2006) Poly(ADP-ribose) (PAR) polymer is a death signal. *Proc Natl Acad Sci USA* 103:18308–18313.
6. Tulin A, Spradling A (2003) Chromatin loosening by poly(ADP)-ribose polymerase (PARP) at *Drosophila* puff loci. *Science* 299:560–562.
7. Petesch SJ, Lis JT (2008) Rapid, transcription-independent loss of nucleosomes over a large chromatin domain at Hsp70 loci. *Cell* 134:74–84.
8. Tulin A, Stewart D, Spradling AC (2002) The *Drosophila* heterochromatic gene encoding poly(ADP-ribose) polymerase (PARP) is required to modulate chromatin structure during development. *Genes Dev* 16:2108–2119.
9. Amé JC, Spenlehauer C, de Murcia G (2004) The PARP superfamily. *BioEssays* 26: 882–893.
10. Adams MD, et al. (2000) The genome sequence of *Drosophila melanogaster*. *Science* 287:2185–2195.
11. Miwa M, Hanai S, Poltronieri P, Uchida M, Uchida K (1999) Functional analysis of poly (ADP-ribose) polymerase in Drosophila melanogaster. *Mol Cell Biochem* 193:103–107.
12. Kameshita I, Matsuda Z, Taniguchi T, Shizuta Y (1984) Poly (ADP-Ribose) synthetase. Separation and identification of three proteolytic fragments as the substrate-binding domain, the DNA-binding domain, and the automodification domain. *J Biol Chem* 259:4770–4776.
13. Kameshita I, Matsuda M, Nishikimi M, Ushiro H, Shizuta Y (1986) Reconstitution and poly(ADP-ribosyl)ation of proteolytically fragmented poly(ADP-ribose) synthetase. *J Biol Chem* 261:3863–3868.
14. Gradwohl G, et al. (1990) The second zinc-finger domain of poly(ADP-ribose) polymerase determines specificity for single-stranded breaks in DNA. *Proc Natl Acad Sci USA* 87: 2990–2994.
15. Wacker DA, et al. (2007) The DNA binding and catalytic domains of poly(ADP-ribose) polymerase 1 cooperate in the regulation of chromatin structure and transcription. *Mol Cell Biol* 27:7475–7485.
16. Artavanis-Tsakonas S (2004) Accessing the Exelixis collection. *Nat Genet* 36:207.
17. Hanai S, et al. (2004) Loss of poly(ADP-ribose) glycohydrolase causes progressive neurodegeneration in *Drosophila melanogaster*. *Proc Natl Acad Sci USA* 101:82–86.
18. Tulin A, Naumova NM, Menon AK, Spradling AC (2006) *Drosophila* poly(ADP-ribose) glycohydrolase mediates chromatin structure and SIR2-dependent silencing. *Genetics* 172:363–371.
19. Pinnola A, Naumova N, Shah M, Tulin AV (2007) Nucleosomal core histones mediate dynamic regulation of poly(ADP-ribose) polymerase 1 protein binding to chromatin and induction of its enzymatic activity. *J Biol Chem* 282:32511–32519.
20. Ji Y, Tulin AV (2009) Poly(ADP-ribosyl)ation of heterogeneous nuclear ribonucleoproteins modulates splicing. *Nucleic Acids Res* 37:3501–3513.
21. Sala A, et al. (2008) The nucleosome-remodeling ATPase ISWI is regulated by poly-ADP-ribosylation. *PLoS Biol* 6:e252.
22. de Murcia JM, et al. (1997) Requirement of poly(ADP-ribose) polymerase in recovery from DNA damage in mice and in cells. *Proc Natl Acad Sci USA* 94:7303–7307.
23. Kotova E, Jarnik M, Tulin AV (2009) Poly (ADP-ribose) polymerase 1 is required for protein localization to Cajal body. *PLoS Genet* 5:e1000387.
24. Sanson B, White P, Vincent JP (1996) Uncoupling cadherin-based adhesion from wingless signalling in *Drosophila*. *Nature* 383:627–630.
25. Mendoza-Alvarez H, Alvarez-Gonzalez R (1993) Poly(ADP-ribose) polymerase is a catalytic dimer and the automodification reaction is intermolecular. *J Biol Chem* 268: 22575–22580.
26. Pion E, et al. (2005) DNA-induced dimerization of poly(ADP-ribose) polymerase-1 triggers its activation. *Biochemistry* 44:14670–14681.
27. Weake VM, Workman JL (2008) Clearing the way for unpaused polymerases. *Cell* 134: 16–18.
28. Kim MY, Mauro S, Gévry N, Lis JT, Kraus WL (2004) NAD+-dependent modulation of chromatin structure and transcription by nucleosome binding properties of PARP-1. *Cell* 119:803–814.
29. Molinete M, et al. (1993) Overproduction of the poly(ADP-ribose) polymerase DNA-binding domain blocks alkylation-induced DNA repair synthesis in mammalian cells. *EMBO J* 12:2109–2117.
30. Dantzer F, Nasheuer HP, Vonesch JL, de Murcia G, Ménissier-de Murcia J (1998) Functional association of poly(ADP-ribose) polymerase with DNA polymerase alpha-primase complex: A link between DNA strand break detection and DNA replication. *Nucleic Acids Res* 26:1891–1898.
31. Krishnakumar R, et al. (2008) Reciprocal binding of PARP-1 and histone H1 at promoters specifies transcriptional outcomes. *Science* 319:819–821.
32. Huang K, et al. (2004) Analysis of nucleotide sequence-dependent DNA binding of poly(ADP-ribose) polymerase in a purified system. *Biochemistry* 43:217–223.
33. Buki KG, Bauer PI, Hakam A, Kun E (1995) Identification of domains of poly(ADP-ribose) polymerase for protein binding and self-association. *J Biol Chem* 270:3370–3377.
34. Poirier GG, de Murcia G, Jongstra-Bilen J, Niedergang C, Mandel P (1982) Poly(ADP-ribosyl)ation of polynucleosomes causes relaxation of chromatin structure. *Proc Natl Acad Sci USA* 79:3423–3427.
35. Aubin RJ, et al. (1983) Correlation between endogenous nucleosomal hyper(ADP-ribosyl)ation of histone H1 and the induction of chromatin relaxation. *EMBO J* 2: 1685–1693.
36. Krupitza G, Cerutti P (1989) Poly(ADP-ribosylation) of histones in intact human keratinocytes. *Biochemistry* 28:4054–4060.